Geochemistry Geophysics Geosystems G3
AN ELECTRONIC JOURNAL OF THE EARTH SCIENCES
Published by AGU and the Geochemical Society

Article
Volume 5, Number 2
26 February 2004
Q02H07, doi:10.1029/2003GC000630
ISSN: 1525-2027

Toward an optimal geomagnetic field intensity determination technique

Yongjae Yu, Lisa Tauxe, and Agnès Genevey

Scripps Institution of Oceanography, La Jolla, California 92093, USA (yjyu@ucsd.edu; ltauxe@ucsd.edu; agenevey@ucsd.edu)

[1] Paleointensity determinations based on double heating techniques (in-field/zero-field cooling, zero-field/in-field cooling, and two in-field steps with opposite laboratory fields) are generally considered to be functionally interchangeable producing equally reliable paleointensity estimates. To investigate this premise, we have developed a simple mathematical model. We find that both the zero-field first and in-field first methods have a strong angular dependence on the laboratory field (parallel, orthogonal, and anti-parallel) while the two in-field steps method is independent of the direction of the laboratory-produced field. Contrary to common practice, each method yields quite different outcomes if the condition of reciprocity of blocking and unblocking temperatures is not met, even with marginal (10%) tails of partial thermoremanence. Our calculations suggest that the zero field first method with the laboratory-produced field anti-parallel to the natural remanence (NRM) is the most robust paleointensity determination technique when the intensity of the lab-induced field is smaller than ancient field. However, the zero field first method with the laboratory-field parallel to the NRM is the optimum approach when the intensity of the lab-induced field is larger than the ancient field. By far the best approach, however, is to alternatethe infield-zerofield (IZ) steps with zerofield-infield (ZI) steps.

Components: 6969 words, 7 figures, 2 tables.

Keywords: Paleointensity; TRM; pTRM; pTRM Tail; Theillier.

Index Terms: 1521 Geomagnetism and Paleomagnetism: Paleointensity; 1594 Geomagnetism and Paleomagnetism: Instruments and techniques; 1500 Geomagnetism and Paleomagnetism.

Received 8 September 2003; **Revised** 17 December 2003; **Accepted** 26 December 2003; **Published** 26 February 2004.

Yu, Y., L. Tauxe, and A. Genevey (2004), Toward an optimal geomagnetic field intensity determination technique, *Geochem. Geophys. Geosyst.*, *5*, Q02H07, doi:10.1029/2003GC000630.

Theme: Geomagnetic Field Behavior Over the Past 5 Myr **Guest Editors:** Cathy Constable and Catherine Johnson

1. Introduction

[2] The geomagnetic field is one of the most intriguing features of the Earth. The Earth's magnetic field originates in the liquid outer core, as a result of electric currents generated by a self-sustaining dynamo. The geomagnetic field is a vector quantity, so that both direction and intensity are required to describe it at any position on the Earth's surface. It is far from being constant either in magnitude or in direction and varies spatially as well as in time. Compared to directional studies, there are far fewer studies on the intensity variations of the geomagnetic field. Geomagnetic field intensity variations are of particular importance because of their direct relevance to the geodynamo,

growth of the inner core, and evolution of core-mantle boundary.

[3] There are a number laboratory protocols for determining absolute paleointensity from geological and archeological materials. The type of method widely considered to be the most reliable involves repeated heating to a given temperature, the so-called Thellier-type geomagnetic field intensity determinations [*Thellier*, 1938; *Thellier and Thellier*, 1959]. These types of experiments rely on the principles of additivity, independence, and reciprocity of partial thermoremanent magnetizations (pTRMs). The principle of independence (see Figure 1) states that a pTRM acquired by cooling in a laboratory field between two temperatures, say 500 and 400°C (pTRM(500, 400)) is independent of a pTRM acquired between two different temperature steps, say pTRM(400, 300). If this is true, then it will also be true that the total TRM acquired by cooling from the Curie temperature to room temperature is equal to the sum of all of the individual pTRMs that would be acquired by cooling between pairs of independent temperature steps spanning the entire temperature range (Figure 1). This is the principle of additivity.

[4] The principle of reciprocity states that a pTRM acquired by cooling from a particular temperature step is entirely removed by heating again to the same temperature step and cooling in zero field. Put another way, reciprocity assumes that the blocking temperature T_b is the same as the unblocking temperature T_{ub}.

[5] The key assumptions of additivity and reciprocity have been experimentally verified for single domain (SD) grains [e.g., *Thellier*, 1938]. However, these assumptions can be violated for somewhat larger grains [see, e.g., *Carlut and Kent*, 2002; *Biggin and Bohnel*, 2003; *Krasa et al.*, 2003; *Yu and Dunlop*, 2003]. In the following, we will denote a pTRM acquired by heating to a specified temperature T_1 and cooling to T_0 $\mathrm{pTRM}_{\uparrow}(T_1, T_0)$. This remanence can often be removed over a range of blocking temperatures as illustrated in Figure 2a. The portion that is removed by reheating to T_1 is the reciprocal portion, denoted $r_{\uparrow}$ and labeled "A" in Figure 2b. The high-temperature tail is approximated by the box labeled "B" in Figure 2b and is denoted $t_{\uparrow}$.

[6] The main advantage of Thellier-type experiments is that a number of tests of the assumptions can be incorporated into the experimental design. Such checks are more difficult in other non-Thellier-type methods [e.g., *Wilson*, 1961; *van Zijl et al.*, 1962; *Smith*, 1967; *Shaw*, 1974; *Walton et al.*, 1992; *Valet and Herrero-Bervera*, 2000].

[7] Detailed reviews of various Thellier-type techniques are given by *Selkin and Tauxe* [2000] and *Valet* [2003]. In the original "Thellier-Thellier" method [*Thellier and Thellier*, 1959], the specimen is heated twice to each of multiple temperature steps, cooling first in a laboratory field $\mathbf{H_{lab}}$, measuring the net remanence and then inverting the specimen and cooling in $-\mathbf{H_{lab}}$ and remeasuring. At each increasing temperature, the NRM is progressively replaced by the pTRMs. At each temperature, the NRM lost can be estimated through vector subtraction.

[8] In practice, the most commonly used technique is the so-called "Coe" method [*Coe*, 1967]. In the Coe method, we first heat the specimen to T_i and cool it in zero field ($\mathbf{H_{lab}} = 0$) to determine the NRM lost directly. Then we heat the specimen again to a given temperature T_i and cool it in a laboratory field ($\mathbf{H_{lab}}$) to determine the pTRM gained.

[9] In order to compensate for something they called "zero field memory effect", *Aitken et al.* [1988] modified the Coe method by reversing the order of the double heatings. In the Aitken method, we impart the pTRM before carrying out zero-field heating [see also *Valet et al.*, 1998].

[10] There are other variants of the Thellier approach. For example, the Kono method [*Kono*, 1974; *Kono and Ueno*, 1977] is another variation of Thellier analysis whereby the specimen is heated (in zero-field) once at each successive temperature T_i and cooled in a laboratory field applied orthogonal to the NRM. Among the various techniques, we are particularly interested in the Aitken, Coe, and Thellier methods because they carry out stepwise double heatings to test reproducibility of pTRMs and they have been used by many research

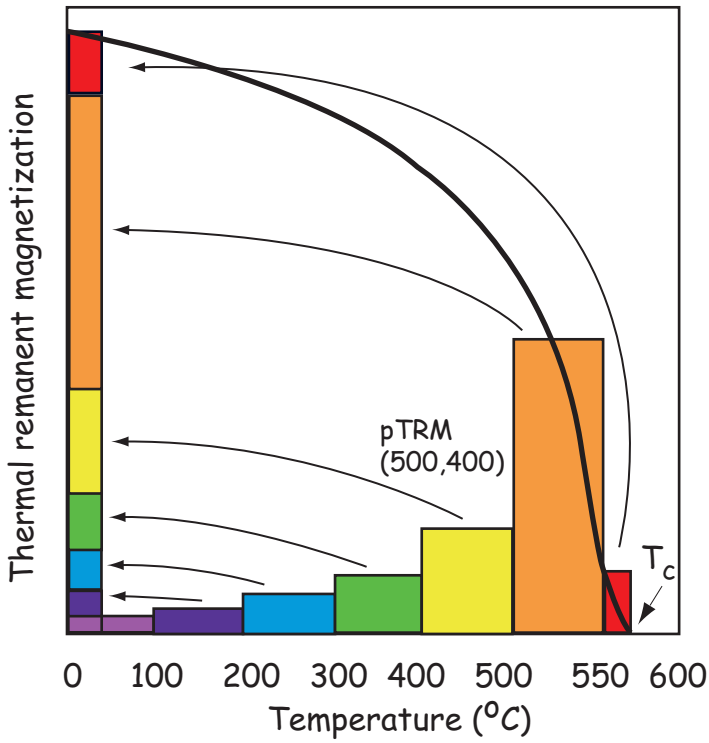

Figure 1. Illustration of the principles of independence and additivity. Independence: the pTRM acquired by cooling between 500 and 400°C, pTRM(500, 400) is independent of that acquired between 400 and 300, or between 600 and 500. Additivity: the total TRM is the sum of the individual pTRM blocks. T_c is the Curie temperature.

groups. In the paleomagnetic community, paleointensity determinations based on these three methods have been considered virtually interchangeable and in fact they are interchangeable as long as the fundamental assumptions hold true. In the present study, we will investigate the performance of these methods under various nonideal conditions, in particular, failure of pTRM reciprocity, to see which is the most effective in detecting and/or compensating for such a failure.

2. Fundamental Properties of pTRM

[11] One necessary condition for a successful paleointensity determination is the validity of the assumption of additivity of pTRM. Additivity of pTRM has been experimentally verified by many authors [*Ozima and Ozima*, 1965; *Dunlop and West*, 1969; *Levi*, 1979; *McClelland and Sugiura*, 1987; *Vinogradov and Markov*, 1989; *Sholpo et al.*, 1991; *Shcherbakova et al.*, 2000; *Dunlop and Özdemir*, 2001]. In particular, *Shcherbakova et al.* [2000] provided an empirical formulation of pTRM additivity based on the blocking/unblocking relation whereby the total TRM acquired by cooling from the Curie Temperature T_c to T_0 is the sum of two pTRMs, one acquired by cooling from T_c to T_1 [$\mathrm{pTRM}_{\downarrow}(T_c, T_1)$] and one acquired by further cooling from T_1 to T_0 [$\mathrm{pTRM}_{\downarrow}(T_1, T_0)$], or:

$$\mathrm{TRM} = \mathrm{pTRM}_{\downarrow}(T_1, T_0) + \mathrm{pTRM}_{\downarrow}(T_c, T_1) \quad (1)$$

[12] For SD grains, a pTRM acquired by cooling from T_1 [$\mathrm{pTRM}_{\downarrow}$ (T_1, T_0)] is removed by heating again to T_1 and cooling in zero field. In the more general case, this principle of reciprocity may be violated. The pTRM may be removed over a range of temperatures extending to temperatures in excess of T_1. We show this schematically in Figure 2c. The portion removed by reheating to T_1 and cooling in zero field is $\mathrm{pTRM}_{\uparrow}$ (T_1, T_0) and the portion that is removed by heating above T_1 is $t_{\downarrow}(T_1 < T_{ub} < T_c)$ (box labeled "C")

$$pTRM_{\downarrow}(T_1, T_0) = pTRM_{\uparrow}(T_1, T_0) + t_{\downarrow}(T_1 < T_{ub} < T_c) \quad (2)$$

where the $\downarrow$ represents an initial state of cooling from T_c to T_1, and the $\uparrow$ represents an initial state

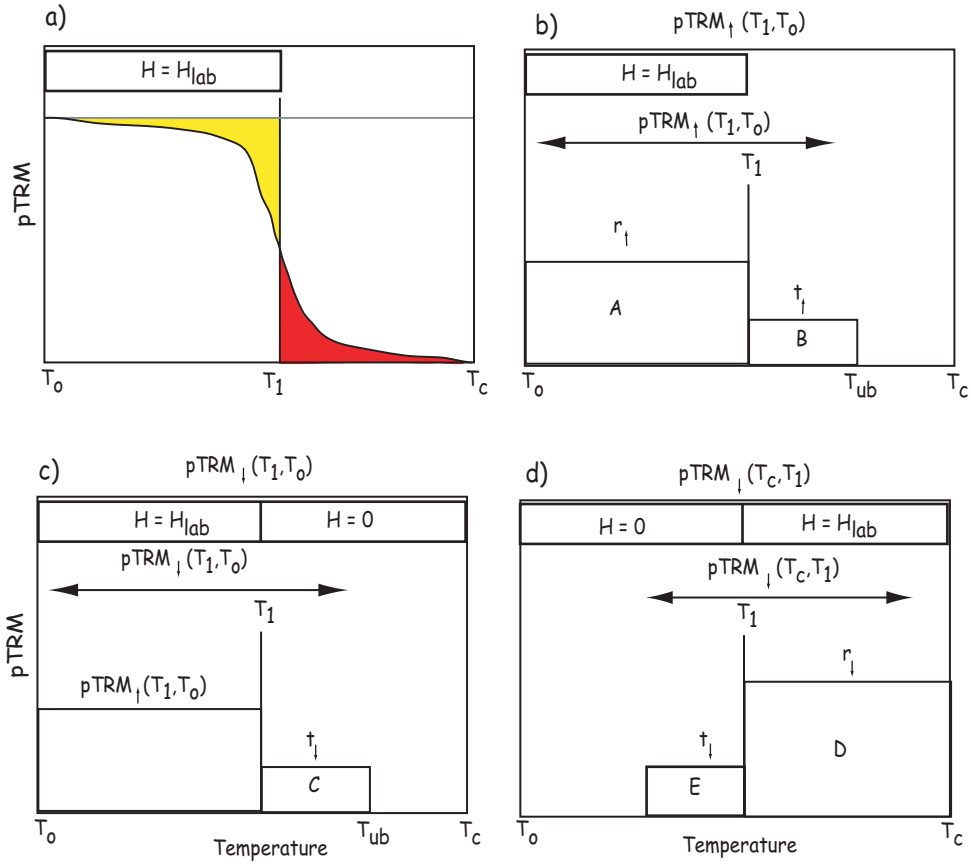

Figure 2. (a) Schematic diagram of thermal demagnetization of a pTRM acquired by heating to T_1 and cooling in a laboratory field H_{lab}. The pTRM has a range of blocking temperatures ranging from well above T_1 (shaded in red) and below T_1 (shaded in yellow). (b)–(d) Three thought experiments imparting pTRM. Partial thermal remanences can be acquired by cooling from the Curie temperature to T_1 (pTRM$_\downarrow$), or by heating to T_1 and cooling in the laboratory field (pTRM$_\uparrow$). Each is composed of a portion for which reciprocity holds (r) and a tail (t) in which $T_{ub} \neq T_b$. These remanence fractions have been labeled A–E for convenience (see text). (b) Thermal demagnetization of pTRM$_\uparrow$(T_1, T_o). pTRM$_\uparrow$ has not only a reciprocal portion $r_\uparrow$, but also a high temperature tail $t_\uparrow$ (labeled "A" and "B" respectively. (c) A specimen is heated to the Curie temperature T_c, then cooled to T_1 in zero field. The field is turned on at T_1 and the specimen is further cooled to T_0. The resulting pTRM$_\downarrow$(T_1, T_0) can be partially remagnetized by reheating to T_1 (pTRM$_\uparrow$(T_1, T_o)) but there is an undemagnetized, high temperature tail ($t_\downarrow$, labeled "C") with T_{ub}($T_1 < T_{ub} < T_c$). (d) A specimen is heated to the Curie temperature T_c and cooled to T_1 in a lab field. The field is then turned off and the specimen is further cooled to T_0. The resulting pTRM$_\downarrow$(T_c, T_1) can be partially demagnetized by reheating to T_1 and cooled in zero field. The pTRM lost thereby is termed the low temperature tail, $t_\downarrow$ (labeled "E"). The remainder of the pTRM can be removed by heating to T_c and is $r_\downarrow$ (labeled "D").

whereby the specimen was reheated to T_1 and cooled to T_0 [*Shcherbakova et al.*, 2000]. The high temperature tail of the pTRM is $t_\downarrow$. The unblocking temperature is T_{ub} and temperatures within parenthesis are blocking temperatures (T_b) for pTRMs and T_{ub} for the tail. To produce a pTRM$_\downarrow$(T_1, T_0), we heat a sample in zero field to the Curie point (T_c) and cool it in zero field to the upper end of the blocking temperature spectrum (T_1) at which point the field is turned on and the specimen cooled to T_0. To produce a pTRM$_\uparrow$(T_1, T_0), we heat the specimen in zero field to T_1 and cool it in a lab field to T_0. If the principle of reciprocity were valid, these two pTRMs would be identical. However, if the unblocking temperature is different from the blocking temperature, these are not the same. In particular, if $T_{ub} > T_b$, pTRM$_\downarrow$(T_1, T_0) will have a tail $t_\downarrow$($T_1 < T_{ub} < T_c$) that is not removed by thermal demagnetization to T_1.

[13] Similarly, a pTRM acquired by cooling from T_c to T_1, $\mathrm{pTRM}_{\downarrow}(T_c, T_1)$, has a low-temperature tail $t_{\downarrow}(T_0 < T_{ub} < T_1)$ that is erased by heating to T_1 (Figure 2d). It also has a fraction for which reciprocity holds (the reciprocal fraction, $r_{\downarrow}(T_1 < T_{ub} < T_c)$) that demagnetizes between T_1 and T_c [*Dunlop and Özdemir*, 2001]. Ergo,

$$\mathrm{pTRM}_{\downarrow}(T_c, T_1) = r_{\downarrow}(T_1 < T_{ub} < T_c) + t_{\downarrow}(T_0 < T_{ub} < T_1). \quad (3)$$

Note that $\mathrm{pTRM}_{\downarrow}(T_c, T_1)$ does not have a high temperature tail because the upper end of the blocking temperatures is T_c. In a similar vein, $\mathrm{pTRM}_{\downarrow}(T_1, T_0)$ lacks a low-temperature tail because the lower end of the blocking temperature is T_0.

[14] We have already noted that $\mathrm{pTRM}_{\uparrow}$ also can have a substantial tail. In practice, because $\mathrm{pTRM}_{\uparrow}$ was acquired in the laboratory field and the $\mathrm{pTRM}_{\downarrow}$ was acquired in the ancient field, the two tails have different directions and may not have the same unblocking temperature spectrum. Therefore $\mathrm{pTRM}_{\uparrow}$ will have a fraction for which reciprocity is valid ($r_{\uparrow}$) and a high temperature tail ($t_{\uparrow}$) as shown in Figure 2b.

[15] The tail $t_{\uparrow}$ in Figure 2b requires us to rewrite equations (1) and (2). Now $\mathrm{pTRM}_{\downarrow}(T_1, T_0)$ is a summation of a reciprocal fraction of the $\mathrm{pTRM}_{\uparrow}$, $r_{\uparrow}(T_0 < T_{ub} < T_1)$, a high-temperature tail of $\mathrm{pTRM}_{\uparrow}$, $t_{\uparrow}(T_1 < T_{Uub} < T_c)$, and a high-temperature tail of $\mathrm{pTRM}_{\downarrow}$, $t_{\downarrow}(T_1 < T_{ub} < T_c)$ (see Figure 2) [*Shcherbakov and Shcherbakova*, 2001; *Yu and Dunlop*, 2003]. We write this as

$$pTRM_{\downarrow}(T_1, T_0) = r_{\uparrow}(T_0 < T_{ub} < T_1) + t_{\uparrow}(T_1 < T_{ub} < T_c) + t_{\downarrow}(T_1 < T_{ub} < T_c). \quad (4)$$

3. Comparison of Double Heating Paleointensity Techniques

3.1. Some Preliminaries

[16] For convenience, we will use the labels as shown in Figure 2: Fraction "A", $r_{\uparrow}(T_o < T_{ub} < T_1)$ of $\mathrm{pTRM}_{\uparrow}(T_1, T_o)$; Fraction "B", $t_{\uparrow}(T_1 < T_{ub} < T_c)$ of $\mathrm{pTRM}_{\uparrow}(T_1, T_o)$; Fraction "C", $t_{\downarrow}(T_1 < T_{ub} < T_c)$ of $\mathrm{pTRM}_{\downarrow}(T_1, T_0)$; Fraction "D", $r_{\downarrow}(T_1 < T_{ub} < T_c)$ of $\mathrm{pTRM}_{\downarrow}(T_c, T_1)$; Fraction "E", $t_{\downarrow}(T_0 < T_{ub} < T_1)$ of $\mathrm{pTRM}_{\downarrow}(T_c, T_1)$.

[17] To clarify our modeling, blocking and unblocking follow the traditional definitions so that zero-field and in-field heating/cooling represent demagnetization and remagnetization processes. For example, the zero-field heating/cooling to T_1 erases the magnetization held by grains with unblocking temperatures $T_{ub} < T_1$, namely fractions A and E. On the other hand, the in-field heating/cooling to T_1 produces $\mathrm{pTRM}_{\uparrow}(T_1, T_0)$, magnetizing/remagnetizing fractions A and B (Figure 2b).

[18] If we consider a Thellier-type double heating experiment at temperature step T_1, the two pTRMs in equations (3) and (4) are needed to describe the experimental process. We also set an initial NRM(=TRM) produced in a field $\mathbf{H_1}$ along z (the cylindrical axis of the sample), so that the NRM has null x and y components and a z component of $A + B + C + D + E$, or in vector notation $[0, 0, A + B + C + D + E]$.

[19] In the Thellier experiment, we replace the NRM with succesive $\mathrm{pTRM}_{\uparrow}$s produced in $\mathbf{H_2}$. $\mathbf{H_2}$ is generally not parallel to $\mathbf{H_1}$ or of equal magnitude. The ratio of the two magnitudes $|H_2|/|H_1|$ is p and the angles relating the two fields are ϕ (in the horizontal plane) and θ (in the vertical plane). For example, the TRM produced in $\mathbf{H_2}$ has a vectorial representation of $(A + B + C + D + E)\, p[\sin\theta\cos\phi, \sin\theta\sin\phi, \cos\theta]$.

3.2. Coe Method

[20] We start with an initial NRM, $\mathbf{M_o}$ = [0, 0, A + B + C + D + E]. The first (zero-field) heating/cooling to T_1 erases fractions A and E, leaving the NRM fraction $\mathbf{M_{C1}}$ = [0, 0, B + C + D]. The second (in-field) heating/cooling to T_1 remagnetizes fractions A and B along $\mathbf{H_2}$, yielding $\mathbf{M_{C2}}$ = $[p(A + B)(\sin\theta\cos\phi), p(A + B)(\sin\theta\sin\phi), p(A + B)(\cos\theta) + C + D]$. Thus the net pTRM acquisition at T_1 is $\mathbf{M_{C2}} - \mathbf{M_{C1}} = [p(A + B)(\sin\theta\cos\phi), p(A + B)(\sin\theta\sin\phi), p(A + B)(\cos\theta) - B]$.

3.3. The pTRM Tail Check

[21] Nonuniformly magnetized grains (so called pseudo-single-domain and multidomain grains)

complicate the paleointensity experiment by violating the principle of reciprocity. Unblocking temperatures larger than the blocking temperature tend to produce a concave downward aspect on Arai-type [*Nagata et al.*, 1963] diagrams. One way of detecting the failure of reciprocity is to carry out an additional zero-field heating following the pTRM acquisition step of the *Coe* method [e.g., *Riisager and Riisager*, 2001]. This third (zero-field) heating/cooling to T_1, sometimes called the pTRM tail check, demagnetizes fraction A but leaves B, yielding $\mathbf{M_{C3}} = [pB(\sin\theta\cos\phi), pB(\sin\theta\sin\phi), pB(\cos\theta) + C + D]$. Thus a nonzero pTRM tail check at T_1 is $\mathbf{M_{C3}} - \mathbf{M_{C1}} = [pB(\sin\theta\cos\phi), pB(\sin\theta\sin\phi), pB(\cos\theta) - B]$.

[22] In practice, such pTRM tail checks have been used to reveal the failure to fully demagnetize a $\text{pTRM}_\uparrow$ acquired at particular temperature step T_1 by reheating and cooling in zero field. This behavior has been interpreted as indicating the presence of multidomain or vortex remanence state particles [e.g., *Riisager et al.*, 2000, 2002; *Riisager and Riisager*, 2001; *Yu and Dunlop*, 2001, 2003; *Carvallo et al.*, 2004; *Tauxe and Love*, 2003].

3.4. Aitken Method

[23] In the Aitken method, in-field heating precedes the zero-field heating step. We start with an initial NRM, $\mathbf{M_0} = [0, 0, A + B + C + D + E]$ as before. The first (in-field) heating/cooling to T_1 erases fraction E and remagnetizes fractions A and B, yielding $\mathbf{M_{A1}} = [p(A + B)(\sin\theta\cos\phi), p(A + B)(\sin\theta\sin\phi), p(A + B)(\cos\theta) + C + D]$. The second (zero field) heating/cooling to T_1 erases fraction A, yielding the NRM remaining at T_1, $\mathbf{M_{A2}} = [pB(\sin\theta\cos\phi), pB(\sin\theta\sin\phi), pB(\cos\theta) + C + D]$. The net pTRM acquired at T_1 is $\mathbf{M_{A1}} - \mathbf{M_{A2}} = [pA(\sin\theta\cos\phi), pA(\sin\theta\sin\phi), pA(\cos\theta)]$.

3.5. Thellier Method

[24] In the classical Thellier method, pairs of in-field (in $\mathbf{H_2}$ and in $-\mathbf{H_2}$) step heatings are carried out. We start with an initial NRM, $\mathbf{M_0} = [0, 0, A + B + C + D + E]$ as before. The first ($\mathbf{H_2}$) heating/cooling to T_1 erases fraction E and remagnetizes fractions A and B, yielding $\mathbf{M_{T1}} = [p(A + B)(\sin\theta\cos\phi), p(A + B)(\sin\theta\sin\phi), p(A + B)(\cos\theta) + C + D]$. The second ($\mathbf{H_2}$) heating/cooling to T_1 remagnetizes fractions A and B in the opposite direction, yielding $\mathbf{M_{T2}} = [-p(A + B)(\sin\theta\cos\phi), -p(A + B)(\sin\theta\sin\phi), -p(A + B)(\cos\theta) + C + D]$. Half of the vector sum of $\mathbf{M_{T1}}$ and $\mathbf{M_{T2}}$ is the NRM remaining at T_1, $[0, 0, C + D]$. Half of the vector difference between $\mathbf{M_{T1}}$ and $\mathbf{M_{T2}}$ is the net pTRM acquisition at T_1, $[p(A + B)(\sin\theta\cos\phi), p(A + B)(\sin\theta\sin\phi), p(A + B)(\cos\theta)]$.

4. Angular Dependence of the Thellier Analysis

[25] In section 3, we have mathematically examined the Aitken, Coe, and Thellier techniques. Results of the NRM remaining and net pTRM acquired at T_1 are summarized in Table 1 for representative cases. To make an easy graphical illustration, $\mathbf{M_1}$ is set to [0, 0, 1] and T_1 is set to be the median destructive temperature (so that $A + B + C = D + E = 0.5$). We assign a magnitude of $\text{pTRM}_\downarrow$ tails (fractions C and E) as 10% of the corresponding pTRMs, ($C = E = 0.05$). Because the $\text{pTRM}_\uparrow$ tail is smaller than $\text{pTRM}_\downarrow$ [see *Shcherbakov and Shcherbakova*, 2001], we set fraction B as half of fraction C, ($B = 0.025$). The remaining reciprocal fractions are accordingly set as $A = 0.425$ and $D = 0.45$. The result is illustrated in an Arai diagram for $p = 0.5$, 1, and 2 (Figure 3). In the case of $\mathbf{H_2} \perp \mathbf{H_1}$, $\mathbf{H_2}$ is set along the x axis. An ideal datapoint ($A = D = 0.5$, $B = C = E = 0$) and an ideal line (perfect reciprocity) are plotted for comparison.

4.1. Coe Method

[26] As shown in section 3.2, $\mathbf{M_{C2}}$ is dependent on the direction of $\mathbf{H_2}$. On the other hand, angular dependence is absent for the NRM remaining ($\mathbf{M_{C1}}$), which is constant regardless of the direction of $\mathbf{H_2}$. In the Coe method, the NRM remaining is always overestimated because $\mathbf{M_{C1}} = [0, 0, B + C + D]$ exceeds 0.5 (Figure 3). If $\mathbf{H_2}$ is anti-parallel to $\mathbf{H_1}$, the Coe method overshoots the ideal line when $\mathbf{H_2}$ is half of $\mathbf{H_1}$. This results from the

Table 1. Representative Thellier Analysis[a]

Method	Net remanence at T_i	$\mathbf{H_2}$ // $\mathbf{H_1}$	$\mathbf{H_2} \perp \mathbf{H_1}$	$\mathbf{H_2}$ \\ $\mathbf{H_1}$
Coe	NRM remaining	[0, 0, $B + C + D$]	[0, 0, $B + C + D$]	[0, 0, $B + C + D$]
Coe	pTRM acquisition	[0, 0, $pA + pB - B$]	[$pA + pB$, 0, $-B$]	[0, 0, $-pA - pB - B$]
Riisager	pTRM tail check	[0, 0, $pB - B$]	[pB, 0, $-B$]	[0, 0, $-pB - B$]
Aitken	NRM remaining	[0, 0, $pB + C + D$]	[pB, 0, $C + D$]	[0, 0, $-pB + C + D$]
Aitken	pTRM acquisition	[0, 0, pA]	[pA, 0, 0]	[0, 0, $-pA$]
Thellier	NRM remaining	[0, 0, $C + D$]	[0, 0, $C + D$]	[0, 0, $C + D$]
Thellier	pTRM acquisition	[0, 0, $pA + pB$]	[$pA + pB$, 0, 0]	[0, 0, $-pA - pB$]

[a] We set fractions $r_{\uparrow}(T_0 < T_{ub} < T_1)$ of $pTRM_{\uparrow}(T_1, T_0)$, $t_{\uparrow}(T_1 < T_{ub} < T_c)$ of $pTRM_{\uparrow}(T_1, T_0)$, $t_{\downarrow}(T_1 < T_{ub} < T_c)$ of $pTRM_{\downarrow}(T_1, T_0)$, $r_{\downarrow}(T_1 < T_{ub} < T_c)$ of $pTRM_{\downarrow}(T_c, T_1)$, and $t_{\downarrow}(T_0 < T_{ub} < T_1)$ of $pTRM_{\downarrow}(T_c, T_1)$ as *A*, *B*, *C*, *D*, *and E*, respectively. Initial NRM(= TRM) is produced in $\mathbf{H_1}$ along *Z* axis of the specimen, so that the NRM has a vectorial representation of [0, 0, $A + B + C + D + E$]. In practice, laboratory-produced field $\mathbf{H_2}$ is not necessarily parallel to $\mathbf{H_1}$. For example, TRM produced in $\mathbf{H_2}$ has a vectorial representation of $(A + B + C + D + E)\,p$ [sinθ cosϕ, sinθ sinϕ, cosθ] where θ is the polar angle between $\mathbf{H_1}$ and $\mathbf{H_2}$, ϕ is the azimuthal angle in the xy-plane from the positive x-axis, and p is the ratio $\mathbf{H_2}/\mathbf{H_1}$.

overestimation of the NRM remaining [0, 0, 0.525], although pTRM acquisition $\mathbf{M_{C2}} - \mathbf{M_{C1}}$ = [0, 0, 0.25] was correctly estimated. It is interesting to note that the Coe method works better than Aitken method when $\mathbf{H_2}$ is larger than $\mathbf{H_1}$. Overall, the Coe method is best suited when the laboratory-induced field ($\mathbf{H_2}$) is anti-parallel to the NRM direction and larger than $\mathbf{H_1}$.

4.2. The pTRM Tail Check

[27] One common confusion in the paleomagnetic community stems from the misunderstanding of the

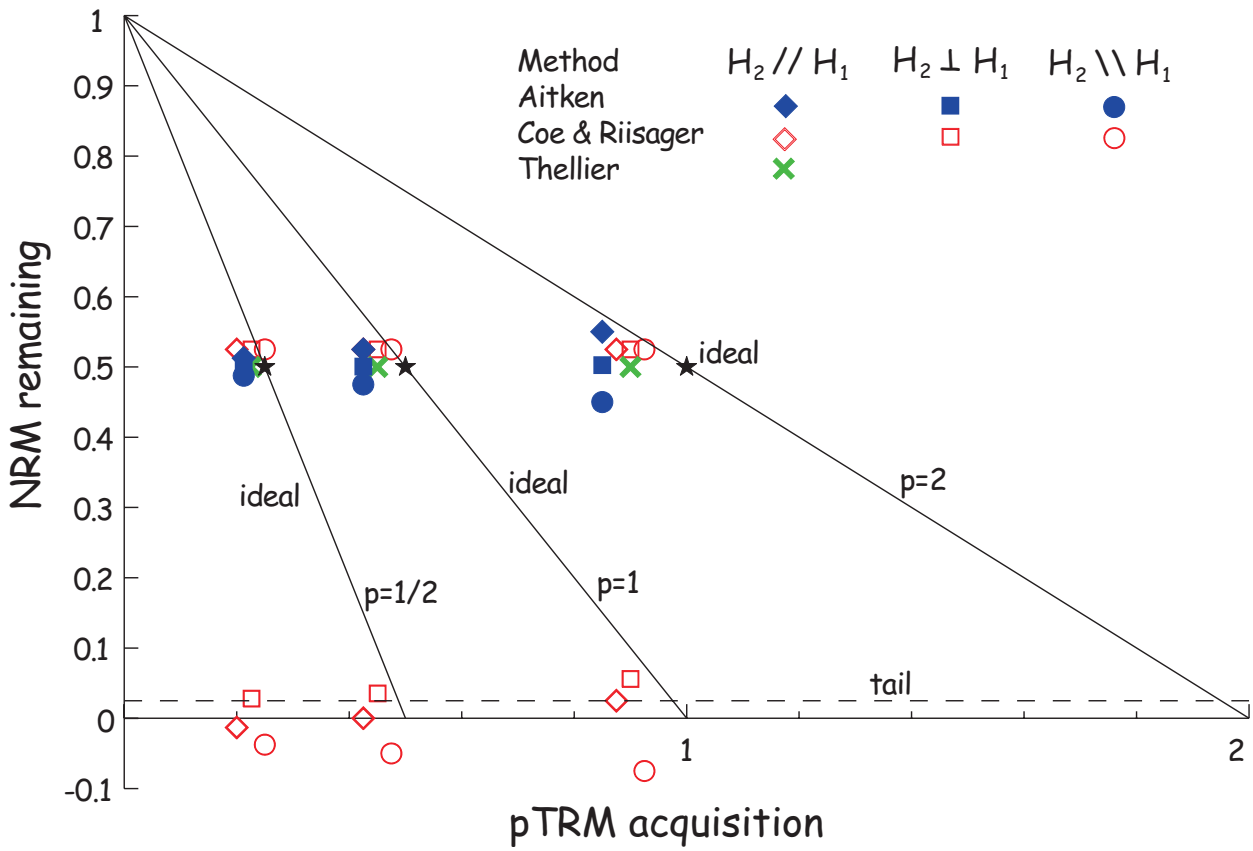

Figure 3. Numerically predicted Arai diagrams for Aitken, Coe, and Thellier methods at temperature step T_i, where T_i was set to be median destructive temperature. We assigned symmetric blocking/unblocking temperature spectrum so that C = E.

two different types of pTRM tails. The pTRM tail check method was designed to detect the $pTRM_{\uparrow}$ tail ($t_{\uparrow}$, B in Figure 2b) and does so. However, it fails to detect reliably the $pTRM_{\downarrow}$ tail ($t_{\downarrow}$, C in Figure 2c [see *Shcherbakov and Shcherbakova*, 2001]). $t_{\downarrow}$ is measurable only when specimens are subjected to heating to the Curie temperature. In other words, although it is embedded in the TRM, the tails of the $pTRM_{\downarrow}$s remain invisible during Thellier analysis, yet can bias the result.

[28] The outcome of our pTRM tail analysis is summarized in Table 2 for some representative situations. In Figure 3, we set a $t_{\uparrow}$ as B = [0, 0, 0.025]. It is surprising that the pTRM tail check detects the proper tail only when $\mathbf{H_2}$ is parallel to and twice as large as $\mathbf{H_1}$. Depending on the direction of $\mathbf{H_2}$ or magnitude of p, the pTRM tail is either overestimated or underestimated. It is interesting that the quality of data in paleointensity determinations improves as $\mathbf{H_2}$ makes a larger angle to the NRM while the pTRM tail is better detected when $\mathbf{H_2}$ is parallel to the NRM (Figure 3). In fact, when $\mathbf{H_2}$ is perpendicular to the NRM, pTRM tails are overestimated while $\mathbf{H_2}$ antiparallel to NRM underestimates tails.

[29] Why does the tail check fail to properly detect the $pTRM_{\uparrow}$ tail? It is not because the $pTRM_{\uparrow}(pB)$ is absent but because pB is masked by a preexisting $pTRM_{\uparrow}$ tail B. Initially the $pTRM_{\uparrow}$ tail was embedded in the total TRM as [0, 0, B]. This inherited fraction systematically deflects pB. In fact, the pTRM tail check analysis detects the vectorial difference between the two ($= \mathbf{M_{C1}} - \mathbf{M_{C1}}$). As a result, the pTRM tail check cannot properly estimate the amount of pB (Figure 3, Table 2).

4.3. Aitken Method

[30] In Figure 3, the Aitken method is always worse than the Thellier method, but often behaves better than the Coe method when $\mathbf{H_2}$ is parallel to the NRM and $p < 1$. When $\mathbf{H_2}$ is larger than $\mathbf{H_1}$, the Aitken method substantially underestimates the pTRM acquisition and shows a significant angular dependence. The only merit that the Aitken method offers is the exact estimate of the NRM remaining when $\mathbf{H_2}$ is perpendicular to NRM (Figure 3).

Table 2. Summary of pTRM Tail Check[a]

p	$\mathbf{H_2} \parallel \mathbf{H_1}$	$\mathbf{H_2} \perp \mathbf{H_1}$	$\mathbf{H_2} \lVert\rVert \mathbf{H_1}$
1	[0, 0, 0]	[B, 0, −B]	[0, 0, −2B]
2	[0, 0, B]	[2B, 0, −B]	[0, 0, −3B]
1/2	[0, 0, −B/2]	[B/2, 0, −B]	[0, 0, −3B/2]

[a] Notations as in Table 1.

4.4. Thellier Method

[31] The Thellier method always yields a precise estimate of the NRM remaining, but underestimates the pTRM acquired (Figure 3). The classical Thellier method is unique in the sense that both pTRM acquisition and NRM remaining are independent of the direction of $\mathbf{H_2}$. It is free from angular dependence because of its experimental design. In the Aitken or Coe methods, tails acquired by laboratory reheating are only affecting the pTRM acquisition steps (in-field heating). On the other hand, in the Thellier analysis, two pTRMs in opposite directions are equally influenced by $pTRM_{\uparrow}$ tails. As a result, the Thellier method is independent of the direction of $\mathbf{H_2}$.

4.5. Further Comparisons

[32] It has been reported that high- and low-temperature tails are roughly symmetric when viscous remanent magnetizations (VRMs) or pTRMs are produced at intermediate (300–400°C) temperatures [*Dunlop and Özdemir*, 2000, 2001]. This interesting observation has been extended to include the entire blocking and unblocking temperature spectrum up to Curie point of magnetite [*Fabian*, 2001; *Shcherbakov and Shcherbakova*, 2001]. However, a symmetric distribution of blocking/unblocking temperature spectra remains to be tested particularly at low (<300°C) and high (>500°C) temperatures. It is therefore worth investigating the outcome of our thought experiments if the high and low temperature tails are not symmetric.

[33] We have assumed symmetry of pTRM tails in Figure 3 so that $C = E = 0.05$, but the total high-temperature tails exceeded a low-temperature tail because of fraction B (= 0.025). Note that symme-

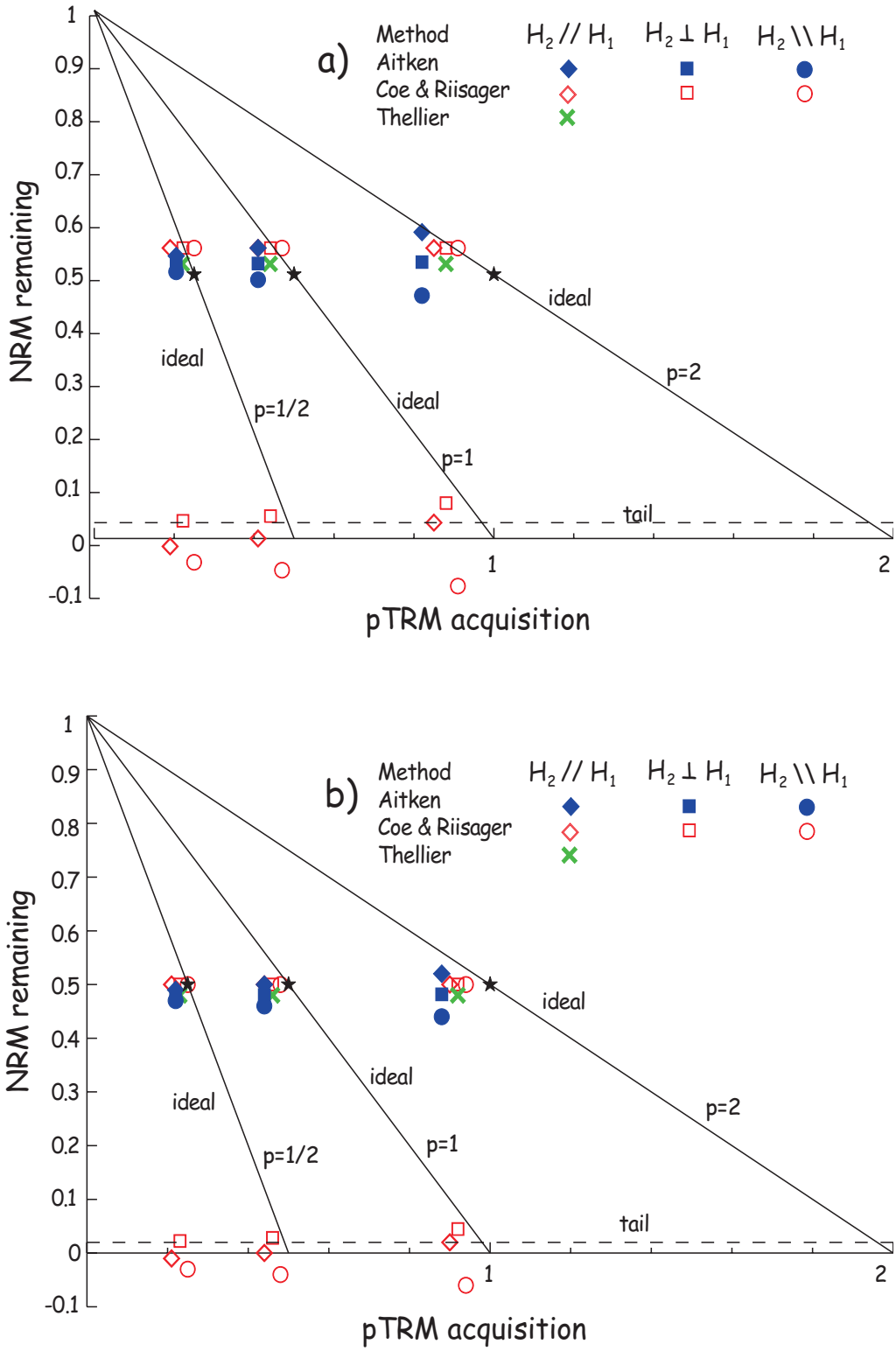

Figure 4. Numerically predicted Arai diagrams for Aitken, Coe, and Thellier methods at temperature step T_i, where T_i was set to be median destructive temperature. In this calculation, we allowed a skewed distribution of unblocking temperature spectrum. (a) B = 0.03, C = 0.06, E = 0.04; (b) B = 0.02, C = 0.04, E = 0.06.

try in rock magnetism represents identical magnitudes between C and E (only for pTRM$_\downarrow$s) and not between $B + C$ and E. In fact, the B fraction has been ignored. In Figure 4, we allowed an asymmetric distribution of the blocking/unblocking relation. At first, we set the high-temperature tails ($B = 0.03$, $C = 0.06$) larger than a low temperature tail ($E = 0.04$) (Figure 4a). Second, a dominant low-temperature tail was set ($B = 0.02$, $C = 0.04$, $E = 0.06$) (Figure 4b). Compared to Figure 3, each datapoint in Figure 4a overestimates the NRM remaining but underestimates the pTRM acquisition. As a result, each datapoint shifts up and to the left in the Arai plot. For a dominant low-temperature tail ($E > C$), underestimation of both NRM remaining and pTRM acquisition worsens, resulting in a more concave down Arai plot (Figure 4b).

5. General Formulations

5.1. Paleointensity Formulations

[34] In sections 3 and 4, a double heating Thellier-type experiment with a single temperature step was investigated. In practical Thellier analyses, we carry out stepwise double heatings at many temperature steps. An empirical formulation of a realistic Thellier experiment is in fact very complicated. For convenience, we adopt a similar convention as in the previous sections so that TRM is produced along the z axis of the specimen. For example, the zero-field heating/cooling to T_i erases the unblocking temperature spectrum ($T_{ub} < T_i$) while in-field heating/cooling to T_i produces a pTRM$_\uparrow$(T_i, T_0). The total TRM is the summation of sequential pTRM$_\downarrow$s:

$$\mathrm{TRM} = \sum_{i=1}^{c} \left[0, 0, \mathrm{pTRM}_\downarrow(T_i, T_{i-1})\right]. \tag{5}$$

According to equation (4), we can generalize equation (5) as follows:

$$TRM = \sum_{i=1}^{c} \left[0, 0, r_\uparrow(T_i, T_{i-1}) + t_\uparrow(T_i, T_{i-1}) + t_{\downarrow 1}(T_i, T_{i-1}) + t_{\downarrow 2}(T_i, T_{i-1})\right] \tag{6}$$

where $r_\uparrow$ is the reciprocal fraction of pTRM$_\uparrow$, $t_\uparrow$ is a high temperature tail of pTRM$_\uparrow$, $t_{\downarrow 1}$ is a high-temperature tail of pTRM$_\downarrow$, $t_{\downarrow 2}$ is a low-temperature tail of pTRM$_\downarrow$, and temperatures within parenthesis are T_bs. Each fraction was sub-divided according to their corresponding unblocking temperature spectrum.

[35] In the Coe method, the first (zero-field) heating and cooling to T_j erases fractions whose unblocking tempartures are less than T_j, leaving the remaining NRM

$$M_{Ci1} = \sum_{i=j+1}^{c} \left[0, 0, r_\uparrow(T_{i-1} < T_{ub} < T_i) + t_{\downarrow 1}(T_{i-1} < T_{ub} < T_i) + t_{\downarrow 2}(T_{i-1} < T_{ub} < T_i)\right] + F. \tag{7}$$

For convenience, we denote the pTRM$_\uparrow$ tail as F,

$$F = \sum_{i=j+1}^{c} \left[0, 0, t_\uparrow(T_{i-1} < T_{ub} < T_i)\right]. \tag{8}$$

[36] The second (in-field) heating/cooling to T_j produces pTRM$_\uparrow$ (T_j, T_0), yielding

$$M_{Ci2} = M_{Ci1} - F + \left(\sum_{i=1}^{j} r_\uparrow(T_{i-1} < T_{ub} < T_i) + \sum_{i=1}^{j} t_\uparrow(T_i, T_{i-1})\right) \cdot [p\sin\theta\cos\phi, p\sin\theta\sin\phi, p\cos\theta]. \tag{9}$$

The net pTRM acquisition at T_j is,

$$M_{Ci2} - M_{Ci1} = \left(\sum_{i=1}^{j} r_\uparrow(T_{i-1} < T_{ub} < T_i) + \sum_{i=1}^{j} t_\uparrow(T_i, T_{i-1})\right) \cdot [p\sin\theta\cos\phi, p\sin\theta\sin\phi, p\cos\theta] - F. \tag{10}$$

In the tail check method, a third (zero field) heating/cooling to T_j yields,

$$M_{Ci3} = M_{Ci1} + \sum_{i=1}^{j} t_\uparrow(T_i, T_{i-1}) \cdot [p\sin\theta\cos\phi, p\sin\theta\sin\phi, p\cos\theta] - F. \tag{11}$$

Thus the measured pTRM tail is,

$$M_{Ci3} - M_{Ci1} = \sum_{i=1}^{j} t_\uparrow(T_i, T_{i-1}) \cdot [p\sin\theta\cos\phi, p\sin\theta\sin\theta, p\cos\theta] - F. \tag{12}$$

[37] As shown in sections 3.4, pTRM acquisition at T_j in the Aitken method is equivalent to $\mathbf{M_{C1}}$ in the Coe method and the NRM remaining at T_j in the Aitken method is equivalent to $\mathbf{M_{C3}}$ in the Coe

method. As a result, in the Aitken method, the NRM lost and the net pTRM acquired at T_j are $\mathbf{M_{Ai2}} = \mathbf{M_{Ci3}}$ and $\mathbf{M_{Ai1}} = \mathbf{M_{Ci2}} - \mathbf{M_{Ci3}}$, respectively.

[38] In the classical Thellier method, the first in-field ($\mathbf{H_2}$) heating yields, $\mathbf{M_{Ti1}} = \mathbf{M_{Ci2}}$. The second in-field ($-\mathbf{H_2}$) heating yields,

$$M_{Ti2} = M_{Ci1} - F - \left(\sum_{i=1}^{j} r_{\uparrow}(T_{ub} < T_i) + \sum_{i=1}^{j} t_{\uparrow}(T_i, T_{i-1})\right) \cdot [p\sin\theta\cos\phi, p\sin\theta\sin\phi, p\cos\theta]. \quad (13)$$

Half of the vector sum of $\mathbf{M_{Ti1}}$ and $\mathbf{M_{Ti2}}$ is the NRM remaining at T_j (= $\mathbf{M_{Ci1}} - F$). Half of the vector difference between $\mathbf{M_{Ti1}}$ and $\mathbf{M_{Ti2}}$ is the net pTRM acquisition at T_j,

$$M_{Ti1} - M_{Ti2} = \left(\sum_{i=1}^{j} r_{\uparrow}(T_{ub} < T_i) + \sum_{i=1}^{j} t_{\uparrow}(T_i, T_{i-1})\right) \cdot [p\sin\theta\cos\phi, p\sin\theta\sin\phi, p\cos\theta]. \quad (14)$$

5.2. Paleointensity Simulation

[39] We now can simulate a more realistic Thellier experiment with four temperature steps. For simplicity, we divide the TRM into five neighboring $pTRM_{\downarrow}$s, each of which has equal intensity. As in the previous sections, we take $t_{\downarrow 1}$ and $t_{\downarrow 2}$ to be 10% each for the corresponding pTRMs. In addition, $t_{\uparrow}$ was set at half of $t_{\downarrow 1}$. Numerically predicted Arai diagrams are presented for p = 0.5, 1, and 2 (Figure 5).

[40] Violation of reciprocity, determined by the difference between each datapoint and the ideal point, diminishes as $\mathbf{H_2}$ makes a larger angle to the NRM for both the Aitken and Coe methods. However, the cumulative effect of pTRM tails causes an underestimation of the pTRM acquisition combined with an overestimation of the NRM remaining, shifting each datapoint up and to the left in the Arai plot. This brings more complexity to our interpretation of an Arai plot. For example, the anti-parallel Aitken method for all p values and the anti-parallel Coe method for $p > 1$ validate reciprocity better than those in the parallel cases, but their data points fall well below the ideal line.

[41] In all simulations, we set fractions $t_{\downarrow 1}$ and $t_{\downarrow 2}$ to 10% of the corresponding pTRMs. When we increased the amount of $pTRM_{\downarrow}$ tails to 30% of the corresponding pTRMs, most conventional methods yield unacceptable results in an Arai plot (Figure 6).

5.3. A New Protocol: The IZZI Method

[42] *Tauxe and Staudigel* [2004] propose a new paleointensity protocol by combining the Aitken (In-field, Zero-field; IZ), and Coe (Zero-field, Infield; ZI), and pTRM tail check methods (called the IZZI method). In this IZZI method, we carry out four heatings (the pTRM check and the pTRM tail check steps) at every other temperature step, while carrying out double heatings (as in the Aitken method) at the intervening temperature steps. (Note, in our thought experiments, which include no alteration, we do not include the pTRM check step.) On the basis of the mathematical analysis in section 5.1, we can predict the outcome of IZZI paleointensity determinations.

[43] Results in the Arai diagram should be zig-zagged if there are significant pTRM tails. This zig-zag pattern would be prominent as the amount of $t_{\uparrow}$ increases (Figure 6) and as $\mathbf{H_2}$ deviates from the NRM direction (Figure 7). As a result, datapoints from the entire IZ steps and those from entire ZI steps will form two different trend lines.

[44] If so, which trend line, the ZI or the IZ results represent the more reliable paleointensity? The answer depends on the direction of $\mathbf{H_2}$ and magnitude of p. In general, the ZI data set yields more reliable paleointensities than that of IZ set. For example, as $\mathbf{H_2}$ deviates from the NRM, a more pronounced concave down feature deelops in the IZ (Aitken) set (Figure 5) than in ZI (Coe) set.

6. Assessing the Classical Paleointensity Protocols

[45] In the paleomagnetic literature, the Aitken, Coe, and Thellier methods are generally thought to yield equally reliable paleointensities. However, this article suggests that this may be true only when specimens satisfy the assumption of reciprocal

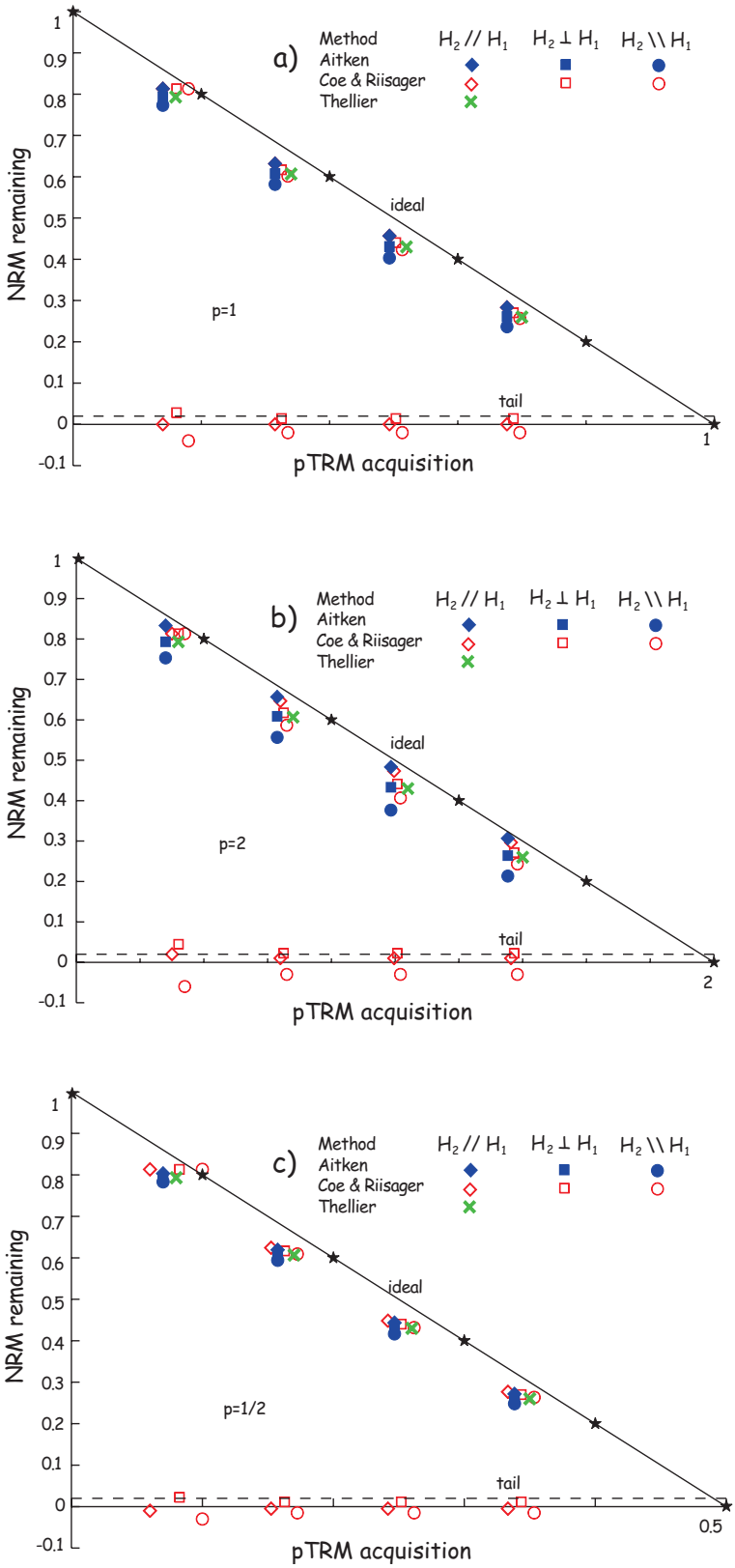

Figure 5. Simulated Arai plots for four-step Thellier analysis. pTRM tails $t_{\downarrow 1}$, $t_{\downarrow 2}$, and $t_{\uparrow}$ are set to be 10%, 10%, and 5% of each corresponding pTRMs. (a) $p = 1$, (b) $p = 2$, (c) $p = 1/2$.

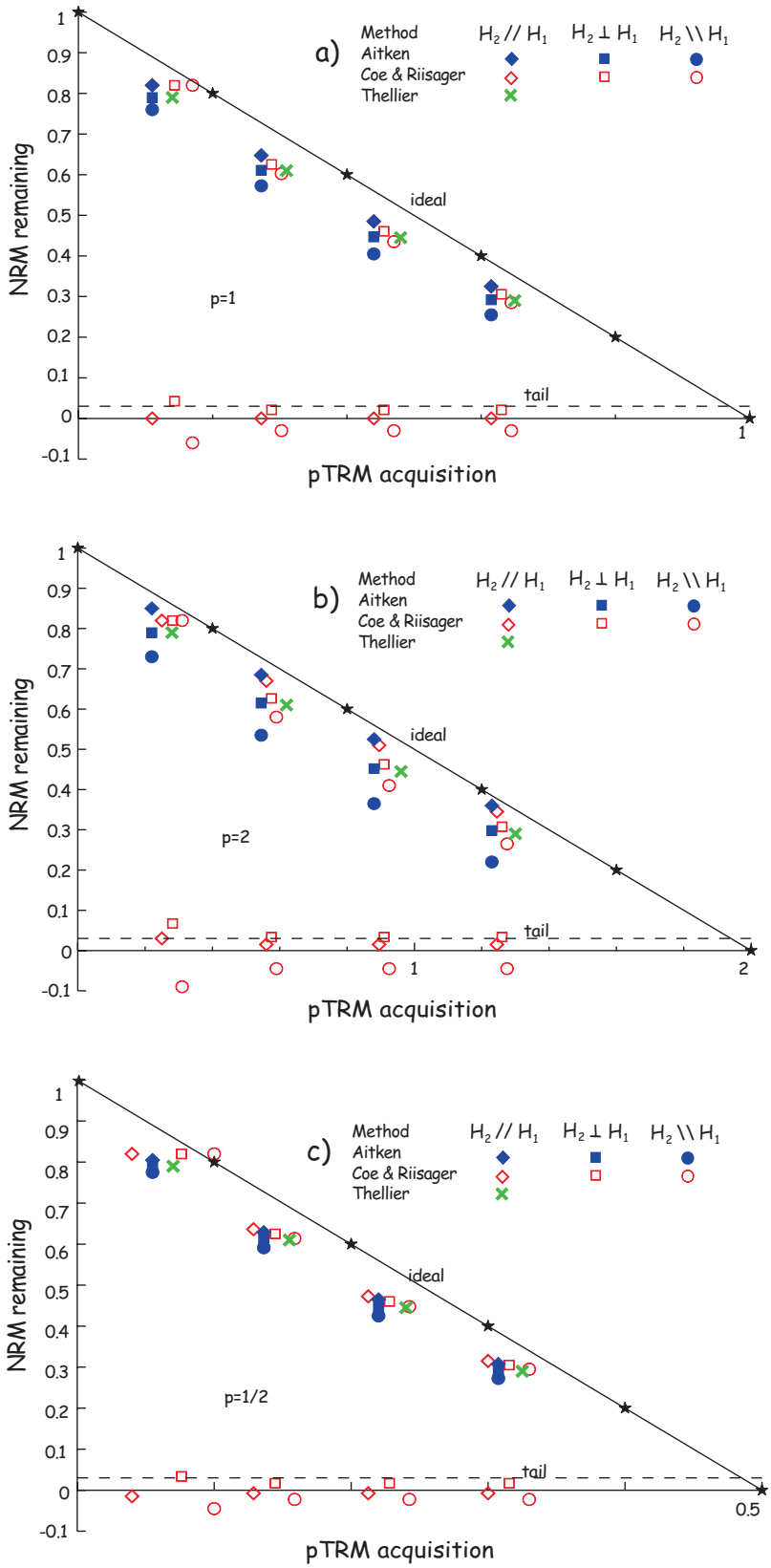

Figure 6. Simulated Arai plots for four-step Thellier analysis. pTRM tails $t_{\downarrow 1}$, $t_{\downarrow 2}$, and $t_{\uparrow}$ are set to be 15%, 15%, and 7.5% of each corresponding pTRMs. (a) $p = 1$, (b) $p = 2$, (c) $p = 1/2$.

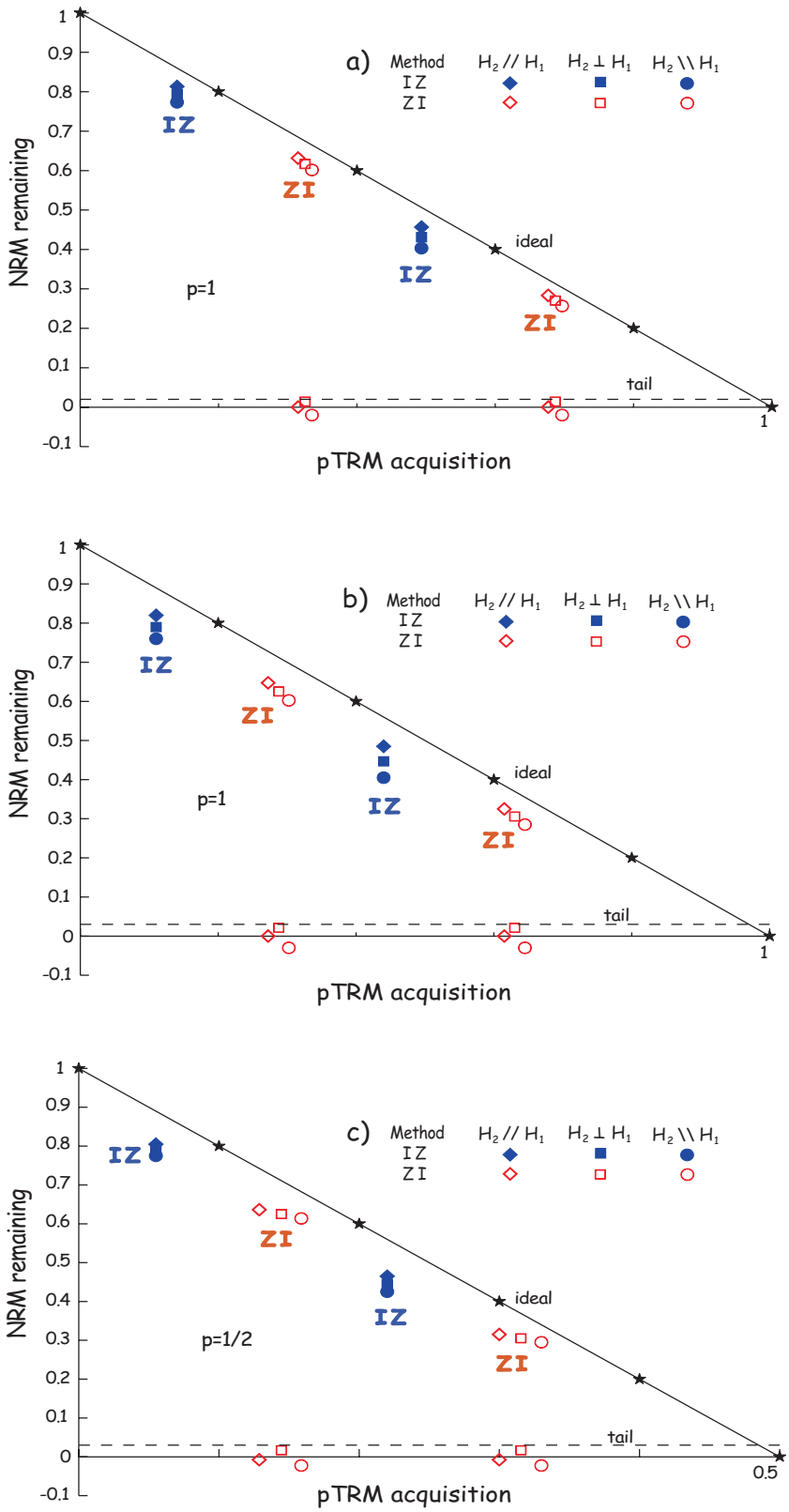

Figure 7. Prediction of Arai plot for IZZI experiments. (a) pTRM tails $t_{\downarrow 1}$, $t_{\downarrow 2}$, and $t_{\uparrow}$ are set to be 10%, 10%, and 5% of each corresponding pTRMs. (b)–(c) pTRM tails $t_{\downarrow 1}$, $t_{\downarrow 2}$, and $t_{\uparrow}$ are set to be 15%, 15%, and 7.5% of each corresponding pTRMs.

blocking and unblocking temperatures. In practice, only uniformly magnetized particles and perhaps also particles whose remanence state is "flower" [see *Schabes and Bertram*, 1988; *Tauxe et al.*, 2002] satisfy reciprocity. Given that many geological specimens have magnetic grains with more complicated remanence states (vortex and multidomain) for which reciprocity may not hold, how can the assumption of reciprocity best be tested in practice?

[46] The use of the Aitken method should be restricted to the case when the magnitude of $\mathbf{H_2}$ is smaller than $\mathbf{H_1}$. When $\mathbf{H_2}$ exceeds $\mathbf{H_1}$, the Aitken method is the least satisfactory among the three techniques considered here. In particular, the Aitken method shows the most angular dependence when $p > 1$ (Figures 3–6).

[47] Only the Thellier method is independent of the direction of $\mathbf{H_2}$ (see section 4.4). Along with the anti-parallel Coe method, the Thellier method detects reciprocity better than other techniques. However, we do not recommend the classical Thellier method because it lacks the pTRM check step (or it requires an extra heating step, while the Aitken and Coe methods require a single in-field heating at each pTRM check step). The pTRM check step is essential to detect alteration of the specimen during the experiment, hence is a requirement in all modern paleointensity investigations.

[48] The Coe method seems to be the most robust technique for practical use of the three classical methods considered here. It is interesting that as the angle between $\mathbf{H_2}$ and NRM increases, reciprocity holds better but the accuracy of detecting proper pTRM tails diminishes (Figures 3–6). In the case of $p > 1$ for parallel Aitken and Coe methods, data points shift nearly along the ideal line, resulting in fairly reliable paleointensity although reciprocity was mostly violated. In other words, depending on the value of p, the angle of $\mathbf{H_2}$ should be determined in Coe method. Perhaps surprisingly, the Coe method works best when $\mathbf{H_2}$ makes a large angle to the NRM for $p < 1$.

[49] An anti-parallel Coe method ($\mathbf{H_2}$ being anti-parallel to NRM) is highly recommended for $p < 1$ to determine the most reliable paleointensity. However, this requires a major correction in modern sample selection criteria. In the nonparallel Coe method, $\text{pTRM}_\uparrow$ tails will likely deflect the NRM toward the direction of $\mathbf{H_2}$. Because both-$\text{pTRM}_\uparrow$ and its tail have a temperature dependence [*Shcherbakov and Shcherbakova*, 2001; *Yu and Dunlop*, 2003], the amount of deflection will vary as the temperature steps change.

[50] Because the pTRM tail has a pronounced angular dependence and can only be detected reliably when $\mathbf{H_2}$ is parallel to the NRM with $p = 2$ (section 4.2), the pTRM tail check is of limited use in practical paleointensity determinations. The conventional pTRM tail check [*Riisager and Riisager*, 2001] detects the vectorial difference between the high-temperature tails of $\text{pTRM}_\uparrow$ and the preexisting high-temperature tails that are embedded in TRM. Therefore the pTRM tail check falls short in its intended purpose.

7. Discussion and Conclusions

[51] In rock magnetism, a linear weak-field dependence of TRM has been thoroughly tested [e.g., *Thellier*, 1938; *Néel*, 1955; *Levi and Merrill*, 1976; *Day*, 1977; *Tucker and Reilly*, 1980; *Shcherbakov et al.*, 1993; *Dunlop and Argyle*, 1997; *Muxworthy and McClelland*, 2000]. On the basis of these experimental confirmations, use of arbitrary p values has been commonly accepted in paleointensity determination as long as $|\mathbf{H_2}|$ is less than $\sim$100 μT. However, on the basis of our mathematical model, results in Tables 1–2 and Figures 3–6 strongly suggest that value of H_2 should be restricted to less than H_1. Otherwise, it is likely to that the paleointensity will be less reliable.

[52] Using $\mathbf{H_2} < \mathbf{H_1}$ has other advantages as well. Within the experimental uncertainty of each data point in real Thellier analyses, it is very likely that the Aitken, Coe, and classical Thellier methods will yield indistinguishable outcomes for specimens with negligible (<10%) $\text{pTRM}_\uparrow$ tails (Figure 3). In practice, however, the angular dependence of the Aitken and Coe techniques are experimentally resolvable when $H_2 > H_1$ (Figures 3 and 4) or when specimens contain substantial tails (Figure 6).

[53] As the amount of the $pTRM_{\uparrow}$ tail increases from 5% (Figure 5) to 7.5% (Figure 6), a more pronounced concave downward feature develops in the Arai diagram. In Figure 6, the paleointensity is demonstrably unreliable in most cases we investigated. In other words, $pTRM_{\uparrow}$ tails more than 5% at any temperature intervals would significantly compromise the quality of paleointensity. Indeed, measuring the $pTRM_{\uparrow}$ tail is a good exercise in preselecting suitable samples for paleointensity determinations, as suggested by *Shcherbakova et al.* [2000] and *Shcherbakov and Shcherbakova* [2001].

[54] The Aitken method is in some respects similar to the pTRM tail check method but does not carry out the first zero field heating. Their physical equivalency is mathematically supported because $\mathbf{M_{A1}} = \mathbf{M_{C2}}$ and $\mathbf{M_{A2}} = \mathbf{M_{C3}}$. However, the outcome on the Arai diagram is quite different. This apparent paradox results not from difference in experimental design but from a difference in data processing. For example, the NRM remaining at T_1 is $\mathbf{M_{A2}}$ in the Aitken method but $\mathbf{M_{C1}}$ in the Coe method (and not $\mathbf{M_{C3}}$) and the pTRM acquisition at T_1 is $\mathbf{M_{A1}} - \mathbf{M_{A2}}$ in the Aitken method but $\mathbf{M_{C2}} - \mathbf{M_{C1}}$ in the Coe method (and not $\mathbf{M_{C2}} - \mathbf{M_{C3}}$).

[55] In section 3.1, we stated that the in-field step at T_1 produces a $pTRM_{\uparrow}$ (T_1, T_0) that magnetize/remagnetizes fractions A and B. There is a possibility that producing a $pTRM_{\uparrow}$ (T_1, T_0) from a demagnetized state and from other partially remagnetized states may induce different pTRMs. Although the initial state dependence of pTRM intensity has been reported [*Shcherbakov et al.*, 2001], its outcome on partially demagnetized/remagnetized samples has not been fully observed. In a similar vein, thermal stability of the pTRM tail [*Shcherbakov and Shcherbakova*, 2001] has raised another puzzle in the context of Thellier experiments. However, any secure conclusion cannot be extracted from the current state of experimental evidence because of the scalar nature of the published experiments where pTRMs are parallel to laboratory produced NRMs. Intensity of pTRM and its tail and the thermal stability of both during Thellier analysis should be analyzed vectorially because pTRM can often be masked/amplified by existing other tails inherited from different magnetization [*Yu and Dunlop*, 2003; this study].

[56] In practical Thellier-type experiments, we do not know the initial field $\mathbf{H_1}$, nor do we know the remanence direction at every step, as the initial NRM may consist of more than one component. Therefore perhaps the best strategy is to have multiple specimens with randomly oriented NRM with respect to the laboratory field $\mathbf{H_2}$. It is also wise to use a relatively low laboratory field, say 10–15 μT, which is lower than most measured paleointensity values. Use of the IZZI protocol under these conditions ensures that reciprocity has been fully tested and that reproducibility among multiple specimens per cooling unit provides a robust estimate for the paleointensity. Relying solely on linearity of the Arai plot, pTRM checks, and even pTRM tail checks is insufficient to guarantee a reliable result.

Acknowledgments

[57] This research was supported by NSF grant EAR0229498 to L. Tauxe. We benefited from fruitful discussions with Peter Selkin. D. V. Kent, V. Shcherbakov, and an anonymous referees provided helpful reviews. We thank Jason Steindorf for help with the measurements.

References

Aitken, M. J., A. L. Allsop, G. D. Bussell, and M. B. Winter (1988), Determination of the intensity of the Earth's magnetic field during archeological times: Reliability of the thellier technique, *Rev. Geophys.*, *26*, 3–12.

Biggin, A. J., and H. N. Bohnel (2003), A method to reduce the curvature of arai plots produced during Thellier paleointensity experiments performed on multidomain grains, *Geophys. J. Int.*, *155*, F13–F19.

Carlut, J., and D. V. Kent (2002), Grain size dependent paleointensity results from very recent mid-oceanic ridge basalts, *J. Geophys. Res.*, *107*(B3), 2049, doi:10.1029/2001JB000439.

Carvallo, C., O. Özdemir, and D. J. Dunlop (2004), Paleointensity determinations, paleodirections, and magnetic properties of basalts from the Emperor seamounts, *Geophys. J. Int.*, *156*, 29–38.

Coe, R. S. (1967), Paleointensities of the Earth's magnetic field determined from Tertiary and Quaternary rocks, *J. Geophys. Res.*, *72*, 3247–5281.

Day, R. (1977), TRM and its variation with grain size, *J. Geomag. Geoelectr.*, *29*, 233–265.

Dunlop, D. J., and K. S. Argyle (1997), Thermoremanence, anhysteretic remanence and susceptibility of submicron magnetites: Nonlinear field dependence and variation with grain size, *J. Geophys. Res*, *102*, 20,199–20,210.

Dunlop, D. J., and O. Özdemir (2000), Effect of grain size and domain state on thermal demagnetization tails, *Geophys. Res. Lett.*, *27*, 1311–1314.

Dunlop, D. J., and O. Özdemir (2001), Beyond Néel's theories: Thermal demagnetization of narrow-band partial thermoremanent magnetization, *Phys. Earth Planet. Int.*, *126*, 43–57.

Dunlop, D. J., and G. F. West (1969), An experimental evaluation of single domain theories, *Rev. Geophys.*, *7*, 709–757.

Fabian, K. (2001), A theoretical treatment of paleointensity determination experiments on rocks containing pseudo-single or multi domain magnetic particles, *Earth Planet. Sci. Lett.*, *188*, 45–48.

Kono, M. (1974), Intensities of the Earth's magnetic field about 60 m.y. ago determined from the Deccan Trap basalts, India, *J. Geophys. Res.*, *79*, 1135–1141.

Kono, M., and N. Ueno (1977), Paleointensity determination by a modified Thellier method, *Phys. Earth Planet. Inter.*, *13*, 305–314.

Krasa, D., C. Heunemann, R. Leonhardt, and N. Petersen (2003), Experimental procedure to detect multidomain remanence during Thellier-Thellier experiments, *Phys. Chem. Earth*, *28*, 681–687.

Levi, S. (1979), The additivity of partial thermoremanent magnetization in magnetite, *Geophys. J.R. Astron. Soc*, *59*, 205–218.

Levi, S., and R. T. Merrill (1976), A comparison of ARM and TRM in magnetite, *Earth Planet. Sci. Lett.*, *32*, 171–184.

McClelland, E., and N. Sugiura (1987), A kinematic model of TRM acquisition in multidomain magnetite, *Phys. Earth Planet. Int.*, *46*, 9–23.

Muxworthy, A., and E. McClelland (2000), The causes of low-temperature demagnetization of remanence in multidomain magnetite, *Geophys. J. Int.*, *140*, 115–131.

Nagata, T., Y. Arai, and K. Momose (1963), Secular variation of the geomagnetic total force during the last 5000 years, *J. Geophys. Res.*, *68*, 5277–5282.

Néel, L. (1955), Some theoretical aspects of rock-magnetism, *Adv. Phys*, *4*, 191–243.

Ozima, M., and M. Ozima (1965), Origin of thermoremanent magnetization, *J. Geophys. Res*, *70*, 1363–1369.

Riisager, P., and J. Riisager (2001), Detecting multidomain magnetic grains in thellier palaeointensity experiments, *Phys. Earth Planet. Inter.*, *125*, 111–117.

Riisager, J., M. Perrin, P. Riisager, and G. Ruffet (2000), Paleomagnetism, paleointensity and geochronology of miocene basalts and baked sediments from Velay Oriental, French Massif Central, *J. Geophys. Res*, *105*, 883–896.

Riisager, P., J. Riisager, N. Abrahamsen, and R. Waagstein (2002), Thellier palaeointensity experiments on faroes flood basalts: Technical aspects and geomagnetic implications, *Phys. Earth Planet. Inter.*, *131*, 91–100.

Schabes, M. E., and H. N. Bertram (1988), Magnetization processes in ferromagnetic cubes, *J. Appl. Phys.*, *64*, 1347–1357.

Selkin, P., and L. Tauxe (2000), Long-term variations in paleointensity, *Philos. Trans. R. Astron. Soc.*, *A358*, 1065–1088.

Shaw, J. (1974), A new method of determining the magnitude of the paleomanetic field application to 5 historic lavas and five archeological samples, *Geophys. J. R. Astron. Soc.*, *39*, 133–141.

Shcherbakov, V. P., and V. Shcherbakova (2001), On the stability of the Thellier method of paleointensity determination on pseudo-single-domain and multidomain grains, *Geophys. J. Int.*, *146*, 20–30.

Shcherbakov, V., E. McClelland, and V. Shcherbakova (1993), A model of multidomain thermoremanent magnetization incorporating temperature-variable domain structure, *J. Geophys. Res*, *98*, 6201–6214.

Shcherbakova, V., V. Shcherbakov, and F. Heider (2000), Properties of partial thermoremanent magnetization in PSD and MD magnetite grains, *J. Geophys. Res*, *105*, 767–782.

Shcherbakov, V. P., V. Shcherbakova, Y. K. Vinogradov, and F. Heider (2001), Thermal stability of pTRM created from different magnetic states, *Phys. Earth Planet. Int.*, *126*, 59–73.

Sholpo, L. E., V. A. Ivanov, and G. P. Borisova (1991), Thermomagnetic effects of reorganization of domain structure, *Izv. Acad. Sci. USSR*, *27*, 617–623.

Smith, P. (1967), The intensity of the Tertiary geomagnetic field, *Geophys. J. Roy. Astron. Soc*, *12*, 239–258.

Tauxe, L., and J. Love (2003), Paleointensity in Hawaiian Scientific Drilling Project Hole (HSDP2): Results from submarine basaltic glass, *Geochem. Geophys. Geosyst.*, *4*(2), 8702, doi:10.1029/2001GC000276.

Tauxe, L., and H. Staudigel (2004), Strength of the geomagnetic field in the Cretaceous Normal Superchron: New data from submarine basaltic glass of the Troodos Ophiolite, *Geochem. Geophys. Geosyst.*, p. in press.

Tauxe, L., H. Bertram, and C. Seberino (2002), Physical interpretation of hysteresis loops: Micromagnetic modelling of fine particle magnetite, *Geochem. Geophys. Geosyst.*, *3*(10), 1055, doi:10.1029/2001GC000241.

Thellier, E. (1938), Sure l'aimantation des teres cuites et ses applications g'eophysique, *Ann. Inst. Phys. Globe Univ. Paris*, *16*, 157–302.

Thellier, E., and O. Thellier (1959), Sur l'intensité du champ magnétique terrestre dans le passé historique et géologique, *Ann. Geophys.*, *15*, 285–378.

Tucker, P., and W. O. Reilly (1980), The acquisition of TRM by MD single crystal titanomagnetite, *Geophys. J. R. Astron. Soc.*, *60*, 21–36.

Valet, J.-P. (2003), Time variations in geomagnetic intensity, *Rev. Geophys.*, *41*(1), 1004, doi:10.1029/2001RG000104.

Valet, J.-P., and E. Herrero-Bervera (2000), Paleointensity experiments using alternating field demagnetization, *Earth Planet. Sci. Lett.*, *177*, 43–58.

Valet, J. P., E. Tric, E. Herrero-Bervera, L. Meynadier, and J. P. Lockwood (1998), Absolute paleointensity from Hawaiian lavas younger than 35 ka, *Earth Planet. Sci. Lett.*, *177*, 19–32.

van Zijl, J. S. U., K. W. T. Graham, and A. L. Hales (1962), The paleomagnetism of the Stormberg lavas, 2. the behavior of the Earth's magnetic field during a reversal, *Geophys. J. R. Astron. Soc.*, *7*, 169–182.

Vinogradov, Y. K., and G. P. Markov (1989), On the effect of low temperature heating on the magnetic state of multidomain magnetite(in Russian), *Investigations in Rock Magnetism and Paleomagnetism*, pp. 31–39, Inst. of Phys. of the Earth, Moscow.

Walton, D., J. Shaw, J. Share, and J. Hakes (1992), Microwave demagnetization, *J. Appl. Phys.*, *71*, 1549–1551.

Wilson, R. L. (1961), Paleomagnetism in northern Ireland: 1, the thermoremanent magnetization of natural magnetic moments in rocks, *Geophys. J. R. Astron. Soc*, *5*, 45–58.

Yu, Y., and D. J. Dunlop (2001), Paleointensity determination on the late precambrian Tudor Gabbro, Ontario, *J. Geophys. Res*, *106*, 26,331–26,344.

Yu, Y., and D. J. Dunlop (2003), On partial thermoremanent magnetization tail checks in Thellier paleointensity determination, *J. Geophys. Res*, *108*(B11), 2523, doi:10.1029/2003JB002420.